Crystal Structure of $Bi_6Sr_{8-x}Ca_{3+x}O_{22}$ ($-0.5 \leq x \leq 1.7$): A Mixed Valence Bismuth Oxide Related to Perovskite

C. C. Luhrs,[†] E. Molins,[†] G. Van Tendeloo,[‡] D. Beltrán-Porter,[§] and A. Fuertes*,[†]

Institut de Ciència de Materials de Barcelona (C.S.I.C.), Campus U.A.B., 08193 Bellaterra, Spain, EMAT, University of Antwerp (RUCA), Antwerp, Belgium, and Institut de Ciència de Materials, Universitat de València, Dr. Moliner 50, 46100 Burjassot, Spain

Received January 21, 1998

The crystal structure of $Bi_6Sr_{8-x}Ca_{3+x}O_{22}$ has been determined by single-crystal X-ray diffraction. This phase is the same as $Bi_9Sr_{11}Ca_5O_y$ that was previously studied by several authors as a secondary phase in the Bi−Sr−Ca−Cu−O system and coexists in thermodynamic equilibrium with the superconductors $Bi_2Sr_2CuO_6$ and $Bi_2Sr_2CaCu_2O_8$. It crystallizes in the monoclinic space group $P2_1/c$, with cell parameters $a = 11.037(3)$ Å, $b = 5.971(2)$ Å, $c = 19.703(7)$ Å, $\beta = 101.46(3)°$, $Z = 2$. The structure was solved by direct methods and full-matrix least-squares refinement. It is built up by perovskite-related blocks of composition $[Sr_{8-x}Bi_2Ca_{3+x}O_{16}]$ that intergrow with double rows $[Bi_4O_6]$ running along b. The perovskite blocks are formed by groups of five octahedra that are shifted from each other $^3/_2\sqrt{2}a_p$ along $[110]_p$ (a_p being the parameter of the cubic perovskite subcell) in a zigzag configuration and are aligned with this direction parallel to the one forming an angle of 25° with the c axis. In turn, the perovskite blocks $[Sr_{8-x}Bi_2Ca_{3+x}O_{16}]$ are shifted from each other $^1/_2$ of both a_p and $\sqrt{2}a_p$ along $[100]_p$ and $[110]_p$, respectively. In the double rows, two trivalent bismuth atoms are placed, forming dimeric anion complexes $[Bi_2O_6]^{6-}$. The oxygen atoms around bismuth in these dimers are placed in the vertexes of a distorted trigonal bipyramid, with one vacant position that would be occupied by the lone pairs characteristic for the electronic configuration of Bi(III). The B sites in the perovskite blocks are occupied by pentavalent bismuth atoms and calcium atoms; the remaining Sr and Ca ions occupy the A sites of the perovskite blocks with coordination numbers with oxygen ranging from 10 to 12. The mean valence for Bi is +3.67 [33.3% of Bi(V) and 66.7% of Bi(III)]. The oxygen vacancies are located in the boundaries between domains having the two possible configurations of the perovskite subcell as in the anionic superconductor $Bi_3BaO_{5.5}$. The oxidation of $Bi_6Sr_{8-x}Ca_{3+x}O_{22}$ at 650 °C allows the complete filling of the oxygen vacancies to form the double perovskite $(Sr_{2-x}Ca_x)Bi_{1.4}Ca_{0.6}O_6$ that shows 92.5% of bismuth in +5 oxidation state. The experimental high-resolution electon microscopy image and the electron diffraction pattern of powder samples along the [010]* zone axis are in good agreement with those calculated from the structural model obtained by single-crystal X-ray diffraction. The material is almost free of defects and the occurrence of planar defects is very exceptional.

Introduction

The study of the relationships and stability ranges of phases in the Bi−Sr−Ca−Cu−O system is of high relevance for the processing of the high-temperature superconductors $Bi_2Sr_2CaCu_2O_8$ and $Bi_2Sr_2Ca_2Cu_3O_{10}$. In the subsystem Bi−Sr−Ca−O, several phases ($Bi_9Sr_{11}Ca_5O_y$, $Bi_2Sr_{1-x}Ca_{1+x}O_y$, $Bi_2Sr_{3-x}Ca_xO_y$, $BiSr_{3-x}Ca_xO_y$) have been identified as impurities during the synthesis of the superconductors,[1−3] and their stability and stoichiometry range have recently been determined.[2−6] The phase $Bi_9Sr_{11}Ca_5O_y$ (so-called 9115) is actually a solid solution for which different stoichiometries have been proposed. It is in thermodynamical equilibrium with the superconductors $Bi_2Sr_2CuO_6$ and $Bi_2Sr_2CaCu_2O_8$, and shows a reversible structural phase transition in oxidizing/reducing atmospheres. In a previous paper we studied the redox processes associated with this transition and determined the crystal structure of the oxidized form of this phase, formulated as $(Sr_{2-x}Ca_x)Bi_{1.4}Ca_{0.6}O_6$ with $0 \leq x \leq 0.5$.[6] It crystallizes in the $P2_1/n$ space group with cell parameters (for $x = 0$) $a = 5.89228(9)$ Å, $b = 5.98928(8)$ Å, $c = 8.38336(14)$ Å, $\beta = 89.946(5)°$ and shows a double perovskite structure with two independent B sites occupied by Ca and Bi that order in a NaCl type arrangement. The same double perovs-

[†] Institut de Ciència de Materials de Barcelona.
[‡] University of Antwerp.
[§] Universitat de València.

(1) Baker, A. P.; Glowacki, B. A. *Physica C* **1994**, *223*, 383.
(2) Rawn, C. J.; Roth, R. S.; Burton, B. P.; Hill, M. D. *J. Am. Ceram. Soc.* **1994**, *77*, 2173.
(3) Müller, R.; Cantoni, M.; Gauckler, L. J. *Phys. C* **1995**, *243*, 103.
(4) Wong-Ng, W.; Roth, R. S. *J. Am. Ceram. Soc.* **1997**, *80*, 324.
(5) Luhrs, C. C.; Morales, M.; Sapiña, F.; Beltrán-Porter, D.; Fuertes, A. *Solid State Ionics* **1998**, *101−103*, 1107.
(6) Luhrs, C.C.; Sapiña, F.; Beltrán-Porter, D.; Casañ-Pastor, N.; Fuertes, A. *J. Mater. Chem.* **1998**, 209.

S0897-4756(98)00037-4 CCC: $15.00
Published on Web 06/13/1998

kite structure but with only bismuth in the B sites can be stabilized at high pressure in the compound $SrBiO_3$ that is rendered superconducting below 12 K upon doping with potasium.[7] In our previous paper, we studied the reduced form of the 9$\underline{11}$5 phase by powder X-ray diffraction, thermal analysis, and electron diffraction. It shows the cell parameters (for $x = 0$) $a = 11.2396(5)$ Å, $b = 5.9097(3)$ Å, $c = 20.0787(9)$ Å, $\beta = 101.747(4)°$ and the space group $P2_1/c$. In this work we present a X-ray single-crystal structure determination and a high-resolution electron microscopy study of this phase that allow us to propose an exact formulation for the corresponding solid solution, $Bi_6Sr_{8-x}Ca_xO_{22}$ ($-0.5 \leq x \leq 1.7$). This represents a new structural type allowing the accommodation of Bi(V) and Bi(III) ions in separated coordination polyhedra that can lead, under oxidation conditions and through a topochemical mechanism, to a pure perovskite structure with 92.5% of bismuth in the +5 oxidation state.

Experimental Section

Synthesis. Powder samples of composition $Sr_2Ca_{0.6}Bi_{1.4}O_{5.2}$ were prepared by the ceramic method, starting with Bi_2O_3 (Aldrich 99.9%), $SrCO_3$ (Baker 99.9%), and $CaCO_3$ (Baker 99.95%). Stoichiometric amounts of the above reactants were mixed and ground in an agate mortar, pelletized, and treated in flowing synthetic air (80% O_2, 20% N_2, Carburos Metálicos, 99.995%) at 800 °C during 120 h with four intermediate regrindings. The purity of the samples was tested by conventional X-ray diffraction and by electron diffraction combined with X-ray energy-dispersive analysis (XEDS).

Needle-shaped single crystals were grown in synthetic air by slow cooling of a previously treated mixture of Bi_2O_3, $SrCO_3$, and $CaCO_3$ in the molar ratio 0.5:0.45:0.55. The powder was placed in a gold crucible and heated to 980 °C at 100 °C/h. This temperature was kept constant during 3 h and then the sample was cooled first at 1 °C/h to 830 °C and second at 100 °C/h from 830 °C to room temperature.

Single-Crystal X-ray Diffraction. A prismatic yellow needle-shaped crystal was selected for the X-ray diffraction experiment. Face indexation (010, 100, 102) was achieved from a top view of the crystal using an equatorial microscope mounted on a Enraf-Nonius CAD4 diffractometer. Cell parameters were $a = 11.037(3)$ Å, $b = 5.971(2)$ Å, $c = 19.703(7)$ Å, $\beta = 101.46(3)°$, $V = 1273$ Å^3. The extinctions in the collected data suggested the $P2_1/c$ monoclinic space group, agreeing with that previously determined on powder samples by electron diffraction.[6] Other crystallographic data are shown in Table 1. The density was calculated assuming $Z = 2$ and the final refined composition of $Bi_6Sr_{6.28}Ca_{4.72}O_{22}$. This corresponds to the member $x = 1.72$ of the solid solution $Bi_6Sr_{8-x}Ca_{3+x}O_{22}$. Data collection parameters and refinement parameters are also provided in Table 1. No decay of the standard reflections was observed. Lorentz, polarization, and absorption corrections were applied in the data reduction. To accurately account for the absorption effects, the Gauss correction was applied for different values of the crystal thickness along the [100] and [102] directions. The values of R_{int} for each pair of $d(100)$ and $d(102)$ thicknesses were fitted to a paraboloid surface. Thus, R_{int} reduces from 0.106, for the uncorrected data set, to 0.071, for the corrected set assuming the measured thicknesses, and to 0.042, for those at the minimum of the paraboloid. These thicknesses (0.026 and 0.022 mm, respectively) are smaller than those previously measured which can be attributed to an overestimation of the absorption coefficient. Some bismuth atoms were located using the SHELX-86 program,[8] and the structure was completed from successive refinement cycles and their corresponding difference Fourier syntheses. At the isotropic stage R_1 values for observed reflections were 0.133 (raw data set) and 0.0808 (optimized data set) and the maximum height values in the residual map were 36.0 and 14.7 e/Å^3, respectively. After the anisotropic refinement (see Table 4), Sr(2) and Sr(4) were allowed to be partially substituted by Ca [Ca(2′) and Ca(4′)]. The final R values were $R_1 = 0.050$ [$F > 4\sigma(F)$, 5112 data], $R_1 = 0.132$ (all independent data, 8914), $wR_2 = 0.125$, GOF = 1.17. Residuals were located near heavy atoms (at distances between 0.4 and 0.9 Å).

Table 1. Crystallographic Data for $Bi_6Sr_{6.28}Ca_{4.72}O_{22}$

temperature	293 K
wavelength	0.71069 Å
crystal system	monoclinic
space group	$P2_1/c$
unit cell dimensions	$a = 11.037(3)$ Å
	$b = 5.971(2)$ Å
	$c = 19.703(7)$ Å
	$\beta = 101.46(3)°$
V (Å^3)	1273
density (calculated)	5.228 g/cm^3
absorption coeficient	55.162 mm^{-1}
$F(000)$	1670
crystal size	0.47 × 0.042 × 0.038 mm
index ranges	$0 < h < 21$, $-8 < k < 11$, $-39 < l < 34$
θ range	$2° \leq 2\theta \leq 45°$
reflections collected (excluding extinctions)	12 758
independent reflections	8914 [R(int) = 0.0417]
data/parameters	8914/181
final R indices [$I > 2\theta(I)$]	$R_1{}^a = 0.0504$, $wR_2{}^b = 0.0854$
extinction coefficient	0.00161(6)
largest diff peak and hole	5.642 and −5.847 e/Å^3

^{a} $R_1 = \sum|F_o - F_c|/\sum F_o$. ^{b} $wR_2 = \sum[w(F_o^2 - F_c^2)^2]/\sum[w(F_o^2)^2]^{1/2}$

High-Resolution Electron Microscopy. Samples for transmission electron microscopy (TEM) were prepared by crushing the powder in ethanol and dispersing the solution on a holey carbon film. High-resolution electron microscopy (HREM) was performed using a JEOL 4000EX instrument with a Scherzer resolution limit of 1.7 Å. For HREM along the monoclinic axis, however, we had to glue the flakes directly on a copper grid, dipped in a soft glue; this was because of the high anisotropy of the material. Computer-simulated images for different defocus and different thicknesses were obtained using the Mactempas program.

Results

Single-Crystal X-ray Diffraction. Atomic coordinates and selected bond distances and angles are listed in Tables 2 and 3, respectively. An ORTEP drawing with the atom-numbering scheme and the projection of the structure along the b axis are shown in Figure 1. The structure is built up from perovskite-related blocks of composition $[Sr_{8-x}Bi_2Ca_{3+x}O_{16}]$ that intergrow with double rows $[Bi_4O_6]$ running along b. The perovskite blocks are formed by groups of five octahedra that are shifted from each other $^3/_2\sqrt{2}a_p$ (a_p being the parameter of the cubic perovskite subcell) along $[110]_p$ in a zigzag configuration and are aligned with this direction parallel to the one forming an angle of 25° with the c axis. In turn, the perovskite blocks $[Sr_{8-x}Bi_2Ca_{3+x}O_{16}]$ are shifted from each other $^1/_2$ of both a_p and $\sqrt{2}a_p$ along $[100]_p$ and $[110]_p$, respectively.

There are three crystallographically independent bismuth atoms. Bi(1) is placed in one of the B sites of

(7) Kazakov, S. M.; Chaillout, C.; Bordet, P.; Capponi, J. J.; Nunez-Regueiro, M.; Rysak, A.; Tholence, J. L.; Radaelli, P. G.; Putilin, S. N.; Antipov, E. V. *Nature* **1997**, *390*, 148.

(8) Sheldrick, G. M. *Acta Crystallogr.* **1990**, *A46*, 467.

Table 2. Atomic Coordinates ($\times 10^4$) and Equivalent Isotropic Displacement Parameters ($Å^2 \times 10^3$) for $Bi_6Sr_{6.28}Ca_{4.72}O_{22}$

atom	x	y	z	Wyckoff site	occ factor	U(eq)
Bi(1)	1213(1)	9924(1)	1526(1)	4e	1	6(1)
Bi(2)	6552(1)	0178(1)	5548(1)	4e	1	10(1)
Bi(3)	5332(1)	5449(1)	4011(1)	4e	1	11(1)
Sr(1)	−524(1)	4527(2)	1743(1)	4e	1	14(1)
Sr(2)	3961(1)	0396(2)	2699(1)	4e	0.68(1)	13(1)
Ca(2')	3961(1)	0396(2)	2699(1)	4e	0.32(1)	13(1)
Sr(3)	−1528(1)	9577(2)	278(1)	4e	1	14(1)
Sr(4)	2619(1)	5276(2)	1221(1)	4e	0.457(9)	10(1)
Ca(4')	2619(1)	5276(2)	1221(1)	4e	0.543(9)	10(1)
Ca(1)	0	5000	0	2b	0.5	7(1)
Ca(2)	−2367(2)	9862(3)	1986(1)	4e	1	7(1)
O(1)	−277(6)	028(1)	2009(4)	4e	1	15(1)
O(2)	2770(7)	949(1)	945(4)	4e	1	16(1)
O(3)	333(6)	193(1)	708(3)	4e	1	10(1)
O(4)	453(7)	715(1)	979(4)	4e	1	14(1)
O(5)	2088(8)	270(1)	2022(4)	4e	1	16(1)
O(6)	−2559(7)	647(2)	1405(4)	4e	1	21(2)
O(7)	−2077(7)	546 (2)	4(4)	4e	1	19(2)
O(8)	4607(7)	425(2)	3042(4)	4e	1	20(2)
O(9)	2276(7)	779(1)	2254(4)	4e	1	14(1)
O(10)	280(1)	676(2)	4061(5)	4e	1	29(2)
O(11)	5384(8)	869(1)	3662(4)	4e	1	20(2)

Table 3. Selected Bond Distances (Å) and Angles (deg) for $Bi_6Sr_{6.28}Ca_{4.72}O_{22}$

Bi(1)−O(1)	2.067(6)	Sr(2)−O(5)	2.618(8)
Bi(1)−O(2)	2.260(7)	Sr(2)−O(6)	2.648(8)
Bi(1)−O(3)	2.087(7)	Sr(2)−O(8)	2.453(8)
Bi(1)−O(4)	2.063(7)	Sr(2)−O(8)	2.461(9)
Bi(1)−O(5)	2.064(7)	Sr(2)−O(9)	2.449(8)
Bi(1)−O(9)	2.095(7)	Sr(2)−O(11)	2.436(8)
Bi(2)−O(6)	2.031(8)	Sr(2)···O(2)	3.489(8)
Bi(2)−O(7)	2.010(9)	Sr(2)···O(8)	3.776(8)
Bi(2)−O(10)	2.055(7)	Sr(2)···O(10)	3.861(9)
Bi(2)−O(11)	2.960(8)	Sr(2)···O(11)	3.513(8)
Bi(3)−O(2)	2.156(7)	Sr(3)−O(2)	2.587(8)
Bi(3)−O(8)	2.050(7)	Sr(3)−O(3)	2.494(7)
Bi(3)−O(10)	2.919(10)	Sr(3)−O(3)	2.709(7)
Bi(3)−O(11)	2.056(8)	Sr(3)−O(4)	2.757(8)
Ca(1)−O(3) × 2	2.290(7)	Sr(3)−O(6)	3.267(9)
Ca(1)−O(4) × 2	2.288(7)	Sr(3)−O(7)	2.551(9)
Ca(1)−O(7) × 2	2.326(8)	Sr(3)−O(10)	2.470(9)
Ca(2)−O(1)	2.318(7)	Sr(3)···O(1)	3.444(7)
Ca(2)−O(5)	2.312(7)	Sr(3)···O(4)	3.540(8)
Ca(2)−O(6)	2.317(9)	Sr(3)···O(7)	3.581(9)
Ca(2)−O(8)	2.489(8)	Sr(4)−O(2)	2.588(8)
Ca(2)−O(9)	2.293(7)	Sr(4)−O(3)	3.221(7)
Ca(2)−O(10)	2.320(9)	Sr(4)−O(4)	2.596(8)
Sr(1)−O(1)	2.485(7)	Sr(4)−O(5)	2.360(8)
Sr(1)−O(1)	2.594(8)	Sr(4)−O(7)	2.478(8)
Sr(1)−O(3)	2.868(7)	Sr(4)−O(9)	2.618(8)
Sr(1)−O(4)	2.553(7)	Sr(4)−O(11)	2.369(9)
Sr(1)−O(5)	3.030(9)	Sr(4)···O(2)	3.505(8)
Sr(1)−O(6)	2.498(8)	Sr(4)···O(8)	3.868(8)
Sr(1)−O(9)	3.198(8)	Sr(4)···O(8)	3.917(8)
Sr(1)−O(10)	3.16(11)		
Sr(1)···O(1)	3.477(7)		
Sr(1)···O(5)	3.762(7)		
Sr(1)···O(7)	3.499(7)		
Sr(1)···O(9)	3.625(7)		
O(6)−Bi(2)−O(7)	93.4(3)	O(2)−Bi(3)−O(8)	98.2(3)
O(6)−Bi(2)−O(10)	92.6(4)	O(2)−Bi(3)−O(10)	175.8(3)
O(6)−Bi(2)−O(11)	87.5(3)	O(2)−Bi(3)−O(11)	99.8(3)
O(7)−Bi(2)−O(10)	97.2(4)	O(8)−Bi(3)−O(10)	85.8(3)
O(7)−Bi(2)−O(11)	176.6(4)	O(8)−Bi(3)−O(11)	92.8(4)
O(10)−Bi(2)−O(11)	80.1(3)	O(10)−Bi(3)−O(11)	81.4(3)

the perovskite-related blocks and shows a low distorted octahedral environment with oxygen atoms. The average metal−oxygen bond length for this polyhedron is 2.11(3) Å. This distance is close to the sum of the ionic radii of Bi^{5+} and O^{2-} ($r_{Bi^{5+}} + r_{O^{2-}}$ (CN=VI) = 2.16 Å).[9] The remaining bismuth atoms, labeled Bi(2) and Bi(3), are placed in the double rows $[Bi_4O_6]$ and show coordination numbers 3 + 1, with three Bi−O bond distances lower than 2.16 Å and a semicoordinated oxygen placed at a distance close to 3 Å. These two environments are typical for bismuth in +3 oxidation state.[10,11] The oxygen atoms around Bi(2) and Bi(3) are placed in the vertexes of a distorted trigonal bipyramid with one vacant position that would be occupied by the lone pair characteristic for the electronic configuration of Bi(III). The bismuth ions in these sites share two oxygen atoms, thus dimerizing to form complex anions $[Bi_2O_6]^{6-}$. The oxygen atoms O(2), O(6), O(7), and O(8) of the dimers are also bonded to bismuth, calcium, and strontium atoms from the perovskite blocks $[Sr_{8-x}Bi_2Ca_{3+x}O_{16}]$ bridging them to the double rows $[Bi_4O_6]$. Considering full occupancy for all oxygen sites [O(1) to O(11)], i.e., a stoichiometry of 22 oxygen atoms per formula unit, the average formal valence calculated for bismuth is +3.67, which is the same than that obtained for two pentavalent bismuth atoms (placed in the perovskite blocks) and four trivalent bismuth atoms (placed in the double rows $[Bi_4O_6]$).

The shifting of the perovskite blocks leads to layers where fragments of BO_2 and AO planes from the perovskite structure ABO_3 coexist (antiphase boundary domains). Figure 2 shows a schematic drawing of two consecutive layers perpendicular to a direction of the cubic perovskite subcell forming an angle of 15° with the *a* axis (see Figure 1). The BO_2 and AO fragments are separated by the double rows $[Bi_4O_6]$, where the oxygen vacancies—with respect to the stoichiometry of a fully oxidized perovskite—are placed. A consequence of the shifting of the perovskite blocks and the existence of oxygen vacancies is the lowering of some of the

Table 4. Anisotropic Temperature Factors ($Å^2 \times 10^3$) for $Bi_6Sr_{6.28}Ca_{4.72}O_{22}$ According to the Expression $\exp(-2\pi^2(h^2(a^*)^2U_{11} + ... + 2hka^*b^*U_{12}))$

atom	U_{11}	U_{22}	U_{33}	U_{23}	U_{13}	U_{12}
Bi(1)	6(1)	5(1)	6(1)	0(1)	0(1)	−1(1)
Bi(2)	6(1)	13(1)	10(1)	−2(1)	0(1)	1(1)
Bi(3)	9(1)	14(1)	9(1)	1(1)	2(1)	3(1)
Sr(1)	16(1)	14(1)	12(1)	3(1)	4(1)	4(1)
Sr(2)	10(1)	14(1)	15(1)	−4(1)	0(1)	1(1)
Ca(2')	10(1)	14(1)	15(1)	−4(1)	0(1)	1(1)
Sr(3)	11(1)	17(1)	15(1)	−6(1)	1(1)	−1(1)
Sr(4)	12(1)	11(1)	9(1)	2(1)	3(1)	4(1)
Ca(4')	12(1)	11(1)	9(1)	2(1)	3(1)	4(1)
Ca(1)	6(1)	10(1)	3(1)	1(1)	0(1)	1(1)
Ca(2)	8(1)	6(1)	7(1)	−2(1)	1(1)	−3(1)
O(1)	7(3)	26(4)	13(3)	2(3)	7(2)	−2(3)
O(2)	12(3)	17(3)	18(3)	−1(3)	4(3)	−2(3)
O(3)	11(2)	8(2)	12(2)	4(1)	2(2)	2(2)
O(4)	14(3)	18(4)	11(3)	−5(3)	1(2)	−6(3)
O(5)	26(4)	5(3)	17(3)	−5(2)	5(3)	−3(3)
O(6)	13(3)	23(4)	25(4)	−8(3)	1(3)	1(3)
O(7)	14(3)	29(4)	17(3)	1(3)	6(3)	−3(3)
O(8)	13(3)	30(4)	16(3)	−15(3)	0(3)	−9(3)
O(9)	13(3)	14(3)	14(3)	9(3)	−2(3)	−1(3)
O(10)	49(6)	19(4)	24(4)	−5(3)	19(4)	−10(4)
O(11)	21(4)	12(3)	25(4)	1(3)	−2(3)	4(3)

(9) Shannon, R. D. *Acta Crystallogr.* **1976**, *A32*, 751.
(10) Wells, A. F. *Structural Inorganic Chemistry*, 5th ed.; The Thedford Press Ltd.: Thedford, United Kingdom, 1984.
(11) Andersson, S.; Åström, A. *Nat. Bur. Stand. Spec. Pub. 364*, Solid State Chemistry, Proceedings of the 5th Material Research Symposium, Vol. 3, 1972.

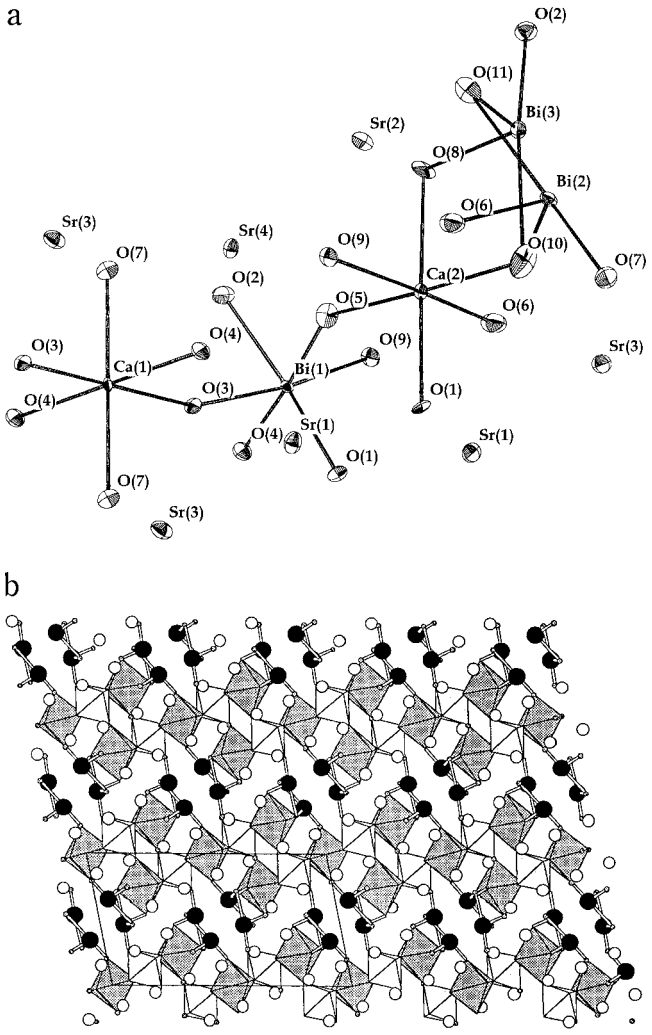

Figure 1. (a) ORTEP drawing and atomic numbering scheme of $Bi_6Sr_{8-x}Ca_{3+x}O_{22}$; (b) projection of the structure of $Bi_6Sr_{8-x}Ca_{3+x}O_{22}$ along [010]. Atom designations: white and gray octahedra represent Bi^{5+} [Bi(1) site] and Ca [Ca(1) and Ca(2) sites] polyhedra, respectively. Bi^{3+} atoms [Bi(2) and Bi(3) sites] are drawn as black spheres, and white spheres correspond to Sr(1), Sr(2), Sr(3), and Sr(4) sites.

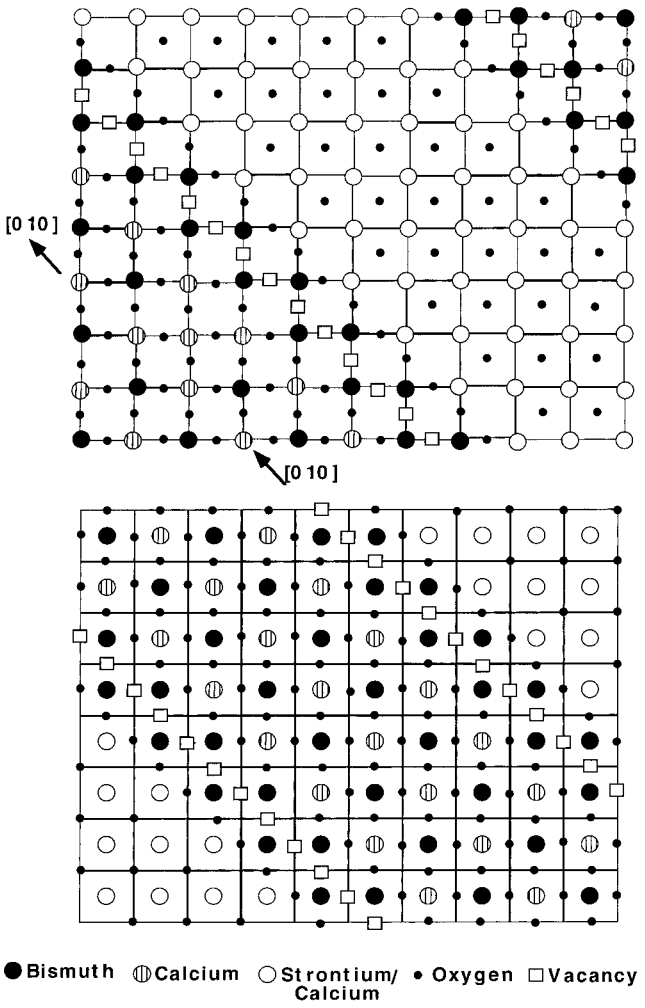

Figure 2. Schematic drawing of two consecutive layers of $Bi_6Sr_{8-x}Ca_{3+x}O_{22}$ perpendicular to a direction of the cubic perovskite subcell forming an angle of 15° with the *a* axis.

coordination numbers for the A sites with respect to that of the perovskite ABO_3. There are four crystallographically independent A sites. Two of them are occupied exclusively by Sr atoms [Sr(1), Sr(3)], the rest being partially occupied by calcium: Sr(2)/Ca(2′) with occupancies 0.68(1)/0.32(1) and Sr(4)/Ca(4′) with occupancies 0.457(9)/0.543(9). The only A site that shows coordination number 12 with oxygen atoms is Sr(1), with eight bond distances between 2.49 and 3.20 Å and four distances between 3.48 and 3.76 Å. The resulting coordination polyhedron is a distorted cuboctahedron. The coordination number for the remaining A sites Sr(2)/Ca(2′), Sr(3), and Sr(4)/Ca(4′) is 10, which is lower than for Sr(1) because these sites are closer to the double rows $[Bi_4O_6]$ (see Figures 1 and 2). The sites occupied partially by Ca, Sr(2), and Sr(4), show a larger number of short bond distances (<2.8 Å) than Sr(3), according to the differences between the ionic radii of Sr and Ca.[9] The Ca ions occupy also two B positions of the perovskite blocks, Ca(1) and Ca(2), showing octahedral coordination with oxygen atoms. The octahedron for Ca(1) is smaller and less distorted than for Ca(2). The average Ca−O distances are respectively 2.301(8) and 2.34(3) Å. The first one is significantly shorter than that expected from the sum of ionic radii (2.39 Å for CN = 6) but it has been also previously observed in perovskites where Ca is occupying the B site, for instance in Ba_2CaIrO_6[12] or $Ba_3CaRu_2O_9$.[13]

High-Resolution Electron Microscopy. The structure of $Sr_8Bi_6Ca_3O_{22}$ has been imaged along different zone axes; the most instructive, however, is along the monoclinic *b*-axis. Because of the large lattice parameters, the experimental images are very much focus dependent; this is evident from the matrix of calculated images as function of thickness and focus (Figure 3). Moreover the material tends to suffer from radiation damage under the intense electron beam used for HREM imaging. This makes a complete through focal series hard to obtain.

The observed [010]* electron diffraction pattern strongly resembles the calculated pattern based on the structural model deduced from the X-ray analysis (Figure 4). The corresponding HREM image of Figure 5 taken close to Scherzer defocus is in relatively good

(12) Jung, D.-Y.; Gravereau, P.; Demazeau, G. *Eur. J. Solid State Inorg. Chem.* **1993**, *30*, 1025.
(13) Wilkens, J.; Müller-Buschbaum, Hk. *Z. Anorg Allg. Chem.* **1993**, *619*, 517.

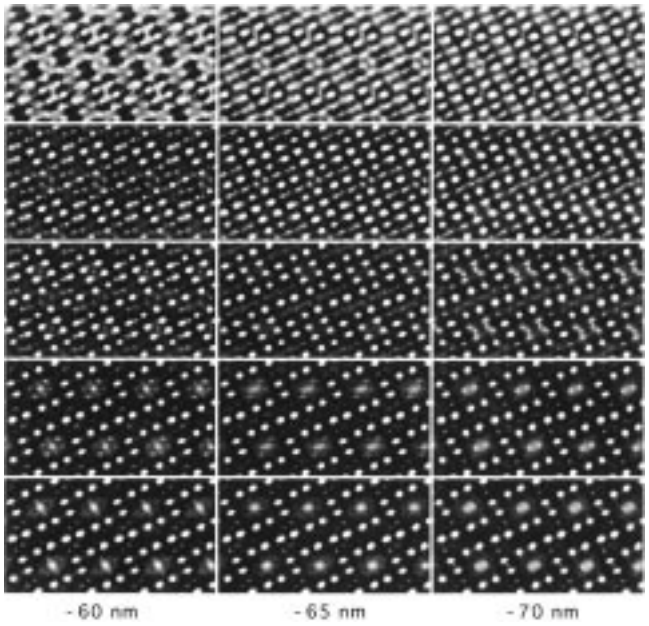

Figure 3. Computer-simulated HREM images of $Bi_6Sr_{8-x}Ca_{3+x}O_{22}$ as function of defocus (−60, −65, and −70 nm) and for variable thicknesses (2, 4, 6, 8, and 10 nm).

agreement with the calculated image for a thickness of 80 Å and a defocus of 600 Å (Figure 6). The intense bright dots in this figure correspond to the Sr configuration, the diffuse maxima corresponding to the open channels between four Bi- ions at $^1/_2a$ and $^1/_2(a + c)$. This can be concluded by superimposing the calculated image of Figure 6 on the projected structure.

The calculations however are not in perfect agreement with the experimental image. Where the calculated images around −60 to −70 nm and for thicknesses between 6 and 10 nm image all Sr atoms with the same intensity, this is clearly not the case in the experimental image of Figure 5. Some Sr atoms clearly have an intensity which is much lower than the others. The material as prepared is almost free of defects and the occurrence of planar defects is very exceptional.

Discussion

As it was stated in the Experimental Section, the single-crystal used in this work for the X-ray diffraction structure determination is the member $x = 1.72$ of the solid solution $Bi_6Sr_{8-x}Ca_{3+x}O_{22}$. In our previous work on the oxidized form of this solid solution, we found that it shows a double perovskite structure with formula $(Sr_{2-x}Ca_x)Bi_{1.4}Ca_{0.6}O_6$ ($0 \le x \le 0.5$) (see Figure 7).[6] In the same work, we showed that the reduced solid solution exists in the same range and it was formulated as well as a double perovskite with the same cationic stoichiometry, but with lower oxygen content, $(Sr_{2-x}Ca_x)Bi_{1.4}Ca_{0.6}O_{5.21}$. Our single crystal structure determination clearly establishes that the reduced solid solution is not purely a double perovskite and leads to the formula $Bi_6Sr_{8-x}Ca_{3+x}O_{22}$ as the true one for the reduced form of the so-called 9$\underline{11}$5 phase. The member with $x = 1.72$ corresponds to the composition $x = 0.5$ for the formulation $(Sr_{2-x}Ca_x)Bi_{1.4}Ca_{0.6}O_{5.21}$ and shows a partial occupation of some of the A sites in the perovskite blocks $[Sr_{8-x}Bi_2Ca_{3+x}O_{16}]$ by calcium atoms. The lower limit of the solid solution we found in our previous work, $x = 0$ for the formulation $(Sr_{2-x}Ca_x)Bi_{1.4}Ca_{0.6}O_{5.21}$, would correspond approximately to the member $x = -0.5$ of the formula $Bi_6Sr_{8-x}Ca_{3+x}O_{22}$ and implies the occupation of 0.5 Sr atoms (0.25 per asymmetric unit) of the B sites in the perovskite blocks $[Sr_{8-x}Bi_2Ca_{3+x}O_{16}]$.

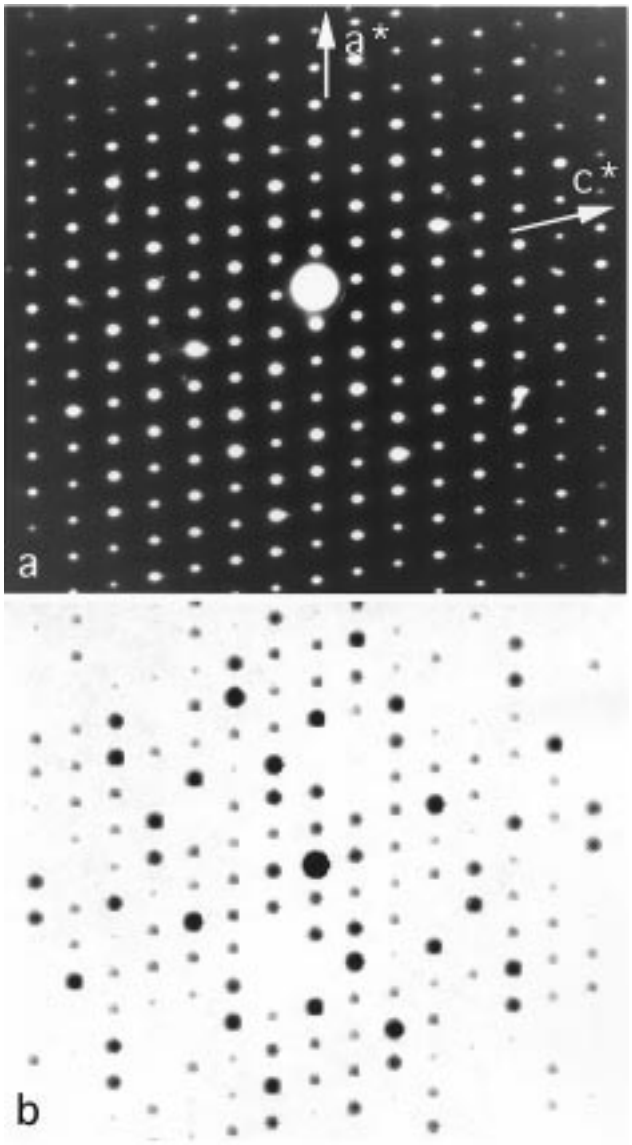

Figure 4. (a) Experimental [010] electron diffraction pattern and (b) computer-simulated pattern.

The formal valence for bismuth found in the present single-crystal X-ray diffraction study is very close to that observed in powder samples of the same phase by iodometric analysis.[6] If we normalize the formula $Bi_6Sr_{8-x}Ca_{3+x}O_{22}$ to 1.4 bismuth atoms, we obtain $(Sr_{1.9-x}Ca_{0.1+x})Bi_{1.4}Ca_{0.6}O_{5.13}$, which can be reformulated as $(Sr_{2-x}Ca_x)Bi_{1.4}\ Ca_{0.6}O_{5.13}$ to fit the cation coefficients of our old formulation. The oxygen content is then almost coincident with 5.20 ± 0.05 that we proposed in our previous work. The oxidation of this phase takes place in oxygen at 650 °C to give the double perovskite structure of $(Sr_{2-x}Ca_x)Bi_{1.4}Ca_{0.6}O_6$. This temperature is high enough to allow the cationic mobility needed to transform one structure into the other. The only mechanism we may propose for this oxidation process is the filling of the oxygen vacancies in the double rows $[Bi_4O_6]$, the almost complete oxidation of these bismuth

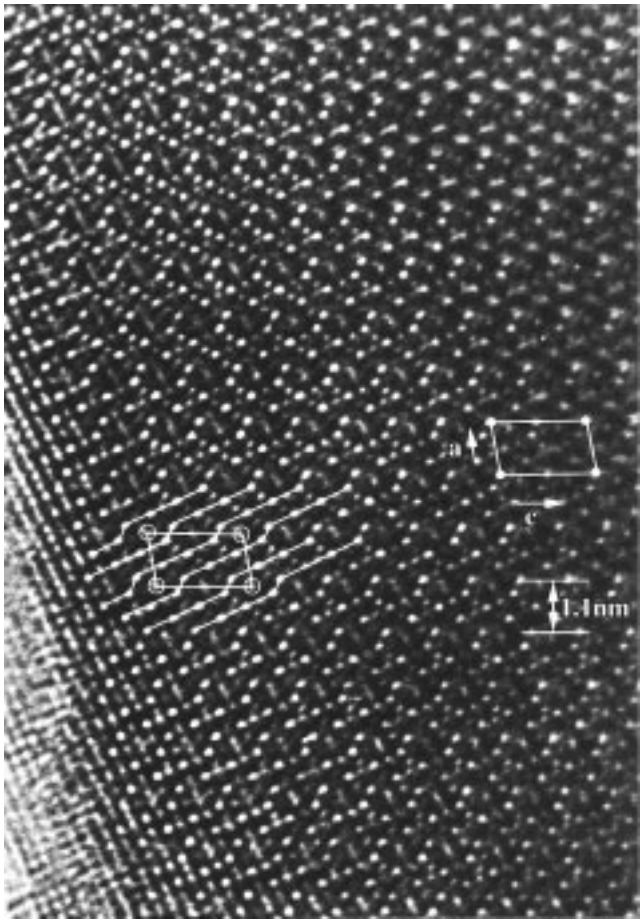

Figure 5. Experimental HREM image of $Bi_6Sr_{8-x}Ca_{3+x}O_{22}$ along [010]; the unit cell has been outlined as well as the rows of Sr-atoms in the structure.

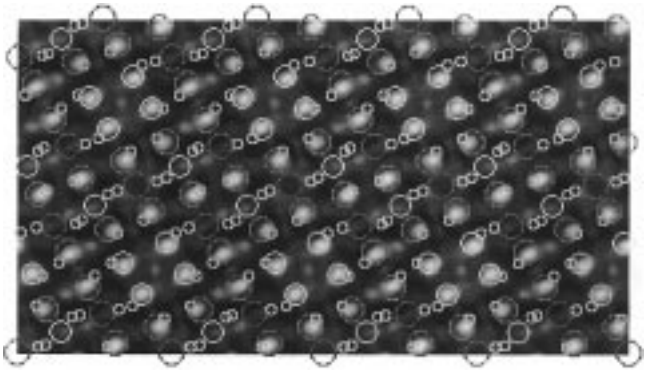

Figure 6. Computer overlay of the projected crystal structure and the computer-simulated image for a thickness of 6 nm and a defocus of −60 nm, identifying the bright dots as the Sr configuration.

atoms to +5 valence state, and the concomitant shifting of the perovskite blocks $[Sr_{8-x}Bi_2Ca_{3+x}O_{16}]$ to give a pure perovskite structure. As in the oxidized phase, the Bi atoms occupy exclusively the B positions of the perovskite; the bismuth ions in the double rows have to move during the oxidation process to these sites. The reduction of the oxidized solid solution takes place in air or oxygen at 800 °C and would be associated to a similar but opposite mechanism. A second redox process that suffers the reduced solid solution is the reduction in Ar/H_2 to a phase with stoichiometry $(Sr_{2-x}Ca_x)Bi_{1.4}Ca_{0.6}O_{4.70}$ and 100% of bismuth in +3 oxidation state.[6] This phase shows a powder X-ray diffraction pattern and electron

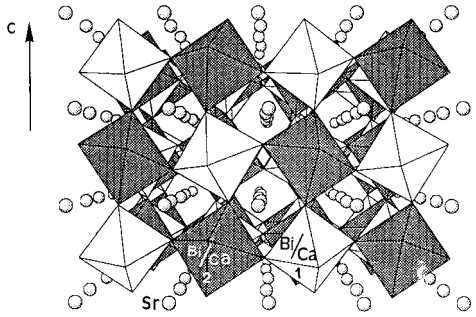

Figure 7. Perspective view of the structure of $Sr_2Bi_{1.4}Ca_{0.6}O_{6.0}$ along a direction close to [110] ($[100]_p$).[6]

diffraction planes similar to $Bi_6Sr_{8-x}Ca_{3+x}O_{22}$. The most remarkable difference is the appearance, in the phase with 4.70 oxygens, of satellite reflections along the direction [110]* of the perovskite subcell. The new formula we propose for that phase is $Bi_6Sr_{8-x}Ca_{3+x}O_{20}$, with the same structure and one oxygen less per asymmetric unit than $Bi_6Sr_{8-x}Ca_{3+x}O_{22}$. As this redox process implies the reduction of the pentavalent bismuth atoms in Bi(1) sites to Bi(III), the most plausible hypotheses for the vacant oxygen are the sites around this position, O(1), O(2), O(3), O(4), O(5), and O(9). The loss of one of these oxygen atoms would also affect to the coordination numbers of the neighboring Bi(2), Bi(3), Ca(1), Ca(2), Sr(1), Sr(2), Sr(3), and Sr(4), giving reasonable coordination polyhedra for these atoms.

The coordination polyhedra of the trivalent bismuth atoms in $Bi_6Sr_{6.28}Ca_{4.72}O_{22}$ are similar to those shown by $Ca_6Bi_6O_{15}$,[14] $BaBiO_{2.5}$,[15] or β-Bi_2O_3.[16] An example of a complex anion similar to $[Bi_2O_6]^{6-}$ has been found in $(Sn_2O_2F_4)Sn_2$, where Sn atoms have also a stereochemically active lone pair of electrons.[17] Among the binary or ternary oxides in the Bi−Sr−Ca−O system that have been fully structurally characterized there are $Ca_4Bi_6O_{13}$,[18] $Ca_6Bi_6O_{15}$,[19] $Sr_2Bi_2O_5$,[20] $CaBi_2O_4$ [21] and more recently, the ternary phase $Bi_{16}Sr_{5+x}Ca_{9-x}O_{38}$.[4,5,22] All of them are Bi(III) phases that do not show apparent relation with the perovskite, excluding $Bi_{16}Sr_{5+x}Ca_{9-x}O_{38}$, where only the cations occupy positions of this structure type.[4,22] In the Bi−Sr−Ca−Cu−O system, a block structure similar to that observed in $Bi_6Sr_{6.28}Ca_{4.72}O_{22}$ has been proposed for the so-called collapsed phases $(Bi_2A_2CuO_6)_{n-2}(Bi_{4+x}A_4Cu_{2-x}O_{12+x/2})$ and $Bi_{16}Sr_{28}Cu_{17}O_{69+\delta}$, from high-resolution electron microscopy studies.[23,24] Our single-crystal structure determination

(14) Parise, J. B.; Torardi, C. C.; Rawn, C. J.; Roth, R. S.; Burton, B. P.; Santoro, A. *J. Solid State Chem.* **1993**, *102*, 132.
(15) Lightfoot, P.; Hriljac, J. A.; Shiyou Pei; Ying Zheng; Mitchell, A. W.; Richards, D. R.; Dabrowski, B.; Jorgensen, J. D.; Hinks, D. G. *J. Solid State Chem.* **1991**, *92*, 473.
(16) Blower, S. K. and Greaves, C. *Acta Crystallogr.* **1988**, *C44*, 587.
(17) Darriet, B. and Galy, J. *Acta Crystallogr.* **1977**, *B33*, 1489.
(18) Parise, J. B.; Torardi, C. C.; Whangbo, M. H.; Rawn, C. J.; Roth, R. S.; Burton, B. P. *Chem. Mater.* **1990**, *2* , 454.
(19) Parise, J. B.; Torardi, C. C.; Rawn, C. J.; Burton, R. S.; Santoro, A. *J. Solid State Chem.* **1993**, *102*, 132.
(20) Torardi, C. C.; Parise, J. B.; Santoro, A.; Rawn, C. J.; Roth, R. S.; Burton, B. P. *J. Solid State Chem.* **1991**, *93*, 228.
(21) Natali ora, I.; Wong-Ng, W.; Huang, Q.; Roth, R. S.; Rawn, C. J.;.Burton, B. P.; Santoro, A. *J. Solid State Chem.* **1994**, *109*, 251.
(22) Luhrs, C. C., Ph.D. Thesis, Universitat Autònoma de Barcelona, December 1997.
(23) Hervieu, M.; Michel, C.; Pham, A. Q.; Raveau, B. *J. Solid State Chem.* **1993**, *104*, 289.
(24) Hervieu, M.; Caldés, M. T.; Cabrera, S.; Michel, C.; Pelloquin, D.; Raveau, B. *J. Solid State Chem.* **1995**, *119*, 169.

shows that the origin of the breaking of the 2201 blocks and the formation of the shearing structure in these phases could be as well some oxygen deficiency and the presence of ribbons of trivalent bismuth ions with a very distorted coordination polyhedra in the boundary zones.

A rich redox behavior has been also observed in the Bi−Sr−O system by Bokhimi et al.[25] The phases $Sr_{10}Bi_6O_{24-y}$ and $Sr_6Bi_2O_{12-y}$ with different oxygen contents show structures based on perovskite, and the X-ray diffraction patterns of the corresponding reduced forms are similar to that shown by $Bi_6Sr_{8-x}Ca_{3+x}O_{22}$. In the Ba−Bi−O system there are also examples of phases that show Bi in a mixed valence state and have structures related to perovskite.[26−31] In both systems, Bi−Sr−O and Bi−Ba−O, the phases with oxygen deficiency with respect to the stoichiometry ABO_3 show superstructure reflections of the cubic perovskite subcell. The phase studied in this paper, $Bi_6Sr_{8-x}Ca_{3+x}O_{22}$, represents a new structural type, allowing the accommodation of Bi(V) and Bi(III) ions in separated coordination polyhedra that can lead, under oxidation conditions and through a topochemical mechanism, to a pure perovskite structure. The reduced phases in the Bi−Sr−O and Ba−Bi−O systems in which the superstructure has not yet been determined could show a similar structure. In fact, for the phase $Bi_3BaO_{5.5}$, a structure with antiphase boundary domains similar to those of $Bi_6Sr_{8-x}Ca_{3+x}O_{22}$ has been proposed.[28] In this oxide, there are oxygen vacancies in the boundaries between domains having the two possible configurations of the perovskite subcell and it shows a high anionic conductivity. The similar crystallochemical features of $Bi_6Sr_{8-x}Ca_{3+x}O_{22}$, together with its rich redox behavior shown in different oxidizing or reducing atmospheres, lead us to think that this phase could also be a good oxygen conductor. A systematic study of the effect of the oxygen stoichiometry on this property at different temperatures is being presently done.

Acknowledgment. This work has been funded by the Spanish CICYT (MAT93-0240-C04 and MAT96-1037-C02), the EC (contract CHRX-CT94-0461), and the Comissionat per Universitats I Recerca de la Generalitat de Catalunya (CIRIT). C.C.L wants to thank the MUTIS program for a fellowship.

CM9800377

(25) Bokhimi; Portilla, M. *J. Solid State Chem.* **1993**, *105*, 371.
(26) Abbatista, F.; Hervieu, M.; Vallino, M.; Michel, C.; Raveau, B. *J. Solid State Chem.* **1993**, *104*, 338.
(27) Michel, C.; Pelloquin, D.; Hervieu, M.; Raveau, B.; Abbatista, F.; Vallino, M. *J. Solid State Chem.* **1994**, *109*, 122.
(28) Licheron, M.; Gervais, F.; Coutures, J.; Choisnet, J. *Solid State Commun.* **1990**, *75*, 759.
(29) Itoh, M.; Sawada, T.; Liang, R.; Kawaji, H.; Nakamura, T. *Solid State Ionics* **1991**, *49*, 57.
(30) Reis, K. P.; Jacobson, A.; Kulik, J. *Chem. Mater.* **1993**, *5*, 1070.
(31) Demourgues, A.; Dussarrat, C.; Bontchev, R.; Darriet, B.; Weill, F.; Darriet, J. *Nuc. Inst. Methods Phys. Res.* **1995**, *B97*, 82.